

$D^0 - \bar{D}^0$ pairs in e^+e^- collisions.

For the neutral D meson system, two mass eigenstates and flavor eigenstates are not equivalent and can be expressed as the following form of the two quantum states:

$$|D_{A,B}\rangle = p|D^0\rangle \pm q|\bar{D}^0\rangle, \quad (1)$$

with eigenvalues of masses and widths to be $m_{A,B}$ and $\Gamma_{A,B}$. Conventionally, the $D^0 - \bar{D}^0$ mixing is described by two small dimensionless parameters:

$$x \equiv \frac{\Delta m}{\Gamma}, y \equiv \frac{\Delta\Gamma}{2\Gamma}, \quad (2)$$

where $\Delta m \equiv m_A - m_B$, $\Delta\Gamma \equiv \Gamma_A - \Gamma_B$ and $\Gamma \equiv (\Gamma_A + \Gamma_B)/2$. The mixing rate R_M is approximately

$$R_M \approx \frac{x^2 + y^2}{2}. \quad (3)$$

In the limit of CP conservation, the $|D_A\rangle$ and $|D_B\rangle$ denote the CP eigenstates.

The mixing parameters can be measured in several ways. The B -factories measured R_M with semileptonic D^0 decay samples^[10, 11]. Reference^[12, 13] also gave an estimation on the sensitivities of R_M measurement at BESIII. Other attempts^[5, 6, 7, 8, 9] are based on the proper-time measurements of the neutral D meson decays. However, the time-dependent analyses are not possible at symmetric charm factory, which operates at the $\psi(3770)$ resonance. In this analysis, we utilize the quantum-coherent threshold production of $D^0 - \bar{D}^0$ pairs in a state of definite $C = -1$. Applying the kinematics of the process of $e^+e^- \rightarrow \psi(3770) \rightarrow D^0\bar{D}^0$, we can reconstruct both neutral D mesons (double tagging (DT) technique) to obtain clean samples to measure the mixing parameters, the strong phase difference and the CP violation. For the single D^0 meson decays into a CP eigenstate, the time-integrated decay rate can be written as^[14, 15]:

$$\Gamma_{CP\pm} \equiv \Gamma(D^0 \rightarrow f_{CP\pm}) = 2A_{CP\pm}^2 [1 \mp y], \quad (4)$$

where $f_{CP\pm}$ is a CP eigenstate with eigenvalue ± 1 , and $A_{CP\pm} \equiv |\langle f_{CP\pm} | \mathcal{H} | D^0 \rangle|$ is the magnitude of decay amplitude. If we consider the coherent D -pair decays, in which one D decays into CP eigenstates and the other D decays semileptonically, the decay rate of $(D^0\bar{D}^0)^{C=-1} \rightarrow (l^\pm X)(f_{CP\pm})$ is described as^[16, 17, 18]:

$$\Gamma_{l,CP} \equiv \Gamma[(l^\pm X)(f_{CP})] \approx A_{l^\pm X}^2 A_{CP}^2, \quad (5)$$

where $A_{l^\pm X} \equiv |\langle l^\pm X | \mathcal{H} | D^0 \rangle|$. Here, we neglect terms to order y^2 or higher since y is much smaller than unit. We, thus, can derive:

$$y = \frac{1}{4} \left(\frac{\Gamma_{l,CP+}\Gamma_{CP-} - \Gamma_{l,CP-}\Gamma_{CP+}}{\Gamma_{l,CP-}\Gamma_{CP+} + \Gamma_{l,CP+}\Gamma_{CP-}} \right). \quad (6)$$

To measure y at BESIII, only the electron channels are used to reconstruct the semileptonic D^0 decays. In the muon channels, the transverse momentum of muon is too low to be efficiently identified by the BESIII muon detector. Thus, the e/π separation plays an essential role to suppress the backgrounds. Fig. 1 shows the momentum distribution of the electrons from the semileptonic D decays. The momentum distribution of the pions from s quark decays is similar to Fig. 1. As a result, the performance of electron identification (e-ID) will determine the precision of the measurement of y parameter.

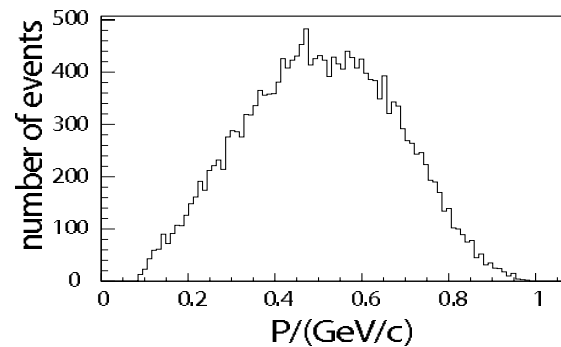


Fig. 1. Momentum of the electron from D^0 semileptonic decays

The designed peak luminosity of BEPCII (Beijing Electron Position Collider) is $10^{33} \text{cm}^{-2} \text{s}^{-1}$ at beam energy $E_{beam} = 1.89 \text{ GeV}$, which is the highest in the tau-charm region ever planned and an unprecedented large number of $\psi(3770)$ events is expected.

This paper is organized as follows: an improved electron identification technique for BESIII is described in Section 2. In Section 3, we describe the method on reconstructing the signals with Monte Carlo (MC) simulation samples. Section 4 presents the estimated sensitivity of y measurement. The summary is presented in Section 5.

2 Electron identification

The BESIII detector operates at BEPCII and consists of a beryllium beam pipe, a helium-based small-celled drift chamber, Time-Of-Flight (TOF) counters for particle identification, a CsI(Tl) crystal electromagnetic calorimeter (EMC), a super-conducting solenoidal magnet with the field of 1 Tesla, and a muon identifier of Resistive Plate Counters (RPC) interleaved with the magnet yoke plates. The BESIII Offline Software System (BOSS)^[19] of version 6.1.0 is used for this analysis. The detector simulation^[20] is based on GEANT4^[21].

The BESIII detector has four subsystems for particle identification: the dE/dx of the main drift

chamber(MDC), TOF, EMC and the muon counter. Among them, the dE/dx and the TOF systems are mainly used for hadron separation, the EMC provides information for electron and photon identification, the MUC has good performance on muon identification^[22].

For electron identification, Refs^[23, 24] illustrate the use of dE/dx of MDC and TOF information. Here, an improved e/π separation technique is introduced in the following sections.

2.1 Electromagnetic calorimeter

The BESIII electromagnetic calorimeter^[22, 25] is composed of one barrel and two endcap sections, covering 93% of 4π . There are a total of 44 rings of crystals along the z direction in the barrel, each with 120 crystals. And there are 6 layers in the endcap, with different number of crystals in each layer. The entire calorimeter has 6240 CsI(Tl) crystals with a total weight of about 24 tons. The energy resolution is expected to be 2.5% and the spatial resolution is expected to be 0.6 cm for 1 GeV/c photon.

The primary function of the EMC is to precisely measure the energies and positions of electron and photon. In order to distinguish electron from hadron, we make use of significant differences in energy deposition and the shower shape of different type of the particles.

2.2 Variables used in e-ID

The following variables are used to identify the electron from pion:

- 1) Ratio of the energy measured by the EMC and the momentum of the charged track by the MDC (E/p).

Ratio of the energy measured by the EMC and the momentum of the charged track by the MDC (E/p). When an electron passes through the calorimeter, the electron produces electromagnetic shower and loses its energy by pair-production, Bremsstrahlung and ionizing/exciting atomic electrons. Since the mass of electron is negligible in the energy range of interest, we expect to have the ratio $E/p = 1$ within the measurement errors. For hadrons, the E/p is typically smaller than one.

- 2) Lateral shower shape at the EMC.

In order to enhance the separation between the electrons and the interacting hadrons, the lateral shower shape can also be utilized. These variables include: $E_{seed}/E_{3\times 3}$, $E_{3\times 3}/E_{5\times 5}$ and the second-moment. Here the E_{seed} is the energy deposited in the central crystal, the $E_{3\times 3}$ and $E_{5\times 5}$ represent the

energy deposit in the 3×3 and 5×5 crystal array, respectively. The second-moment S is defined as

$$S = \frac{\sum_i E_i \cdot d_i^2}{\sum_i E_i}, \quad (7)$$

where E_i is the energy deposit in the i -th crystal, and d_i is the distance between the i -th crystal and the center position of reconstructed shower. Detailed description of E/p and the lateral shower shape can be found in Ref^[23].

3) Longitudinal shower shape at the EMC.

The longitudinal shower shape provides additional information for electron identification. The variable $\Delta\phi$, between the polar angles where the track intersects the EMC and the shower center, can be used. The distributions of $\Delta\phi$ for electron and pion are drawn in Fig. 2. The center of electron showers is closer to the impact point of track on EMC since the electron showers reach their maximum earlier than hadrons.

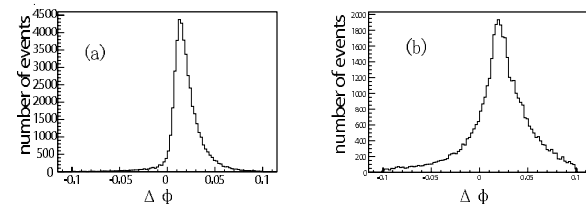


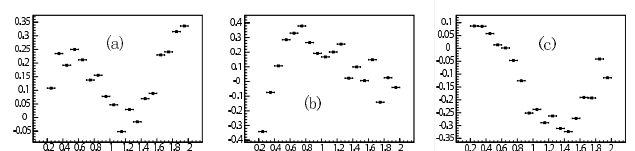
Fig. 2. $\Delta\phi$ of (a) electron (b) pion.

2.3 The correlation between variables

The E/p ratio, lateral shower shape and longitudinal shower shape are all depending on the deposited energy in the crystals. Thus, these variables may be correlated. We calculate the correlation coefficients ρ_{ij} between the E/p , $E_{3\times 3}/E_{5\times 5}$ and $\Delta\phi$ using the function:

$$M_{i,j} = \sum_{i,j} (x_i - \bar{x}_i) \cdot (x_j - \bar{x}_j), \quad \rho_{ij} = \frac{M_{ij}}{\sqrt{M_{ii} \times M_{jj}}}, \quad (8)$$

where i, j are the indices of the variable names. Figure. 3 shows the correlation between any two of the variables of electron and pion, respectively, with the momentum ranging from 0.2 GeV/c to 2.0 GeV/c. Here, the x-axis represents the particle momentum and the y-axis represents the correlation coefficient ρ_{ij} . The distribution indicates strong correlation between the variables.



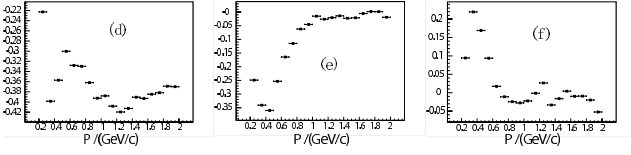


Fig. 3. Correlations between (a)E/p and $E_{seed}/E_{3\times 3}$ of electron; (b)E/p and $E_{3\times 3}/E_{5\times 5}$ of electron; (c) $E_{seed}/E_{3\times 3}$ and $E_{3\times 3}/E_{5\times 5}$ of electron; (d)E/p and $E_{seed}/E_{3\times 3}$ of pion; (e)E/p and $E_{3\times 3}/E_{5\times 5}$ of pion; (f) $E_{seed}/E_{3\times 3}$ and $E_{3\times 3}/E_{5\times 5}$ of pion.

2.4 PID Algorithm

Considering the correlations between the variables, the traditional method for particle identification may be underperforming. In the e-ID, we implement the artificial neural network (ANN) [26] to provide a general framework for estimating non-linear functional mapping between the input variables and the output variable. For the neural network (NN) training, we use the momentum, traverse momentum and other six discriminants (total deposit energy, E_{seed} , $E_{3\times 3}$, $E_{5\times 5}$, second moment and $\Delta\phi$) as the input variables. The network we choose has one hidden layer with 16 neurons and one output value. Figure. 4 shows the two-dimension distributions of the output value versus the momentum of the electrons and pions. It is obvious that the distribution of the output value depends on the momentum, especially at low momentum region. Thus, it is unsuitable to apply a single cut on the output value to separate the electrons from the pions. In practice, we construct probability density function (PDF) of the NN output value at every 0.1 GeV/c momentum bin. The PDF is obtained from fitting the nearest 4 bins of the NN output value, with the third-order polynomial function. Then, the PDF value of the NN output can be extracted from the fit. Finally, we make the PID decision by comparing the likelihood values of electron and pion hypothesis.

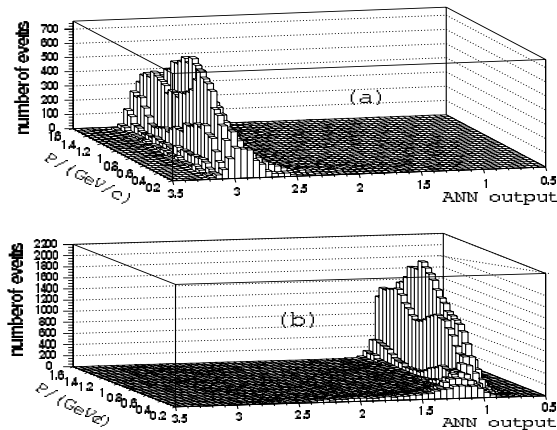


Fig. 4. The NN outputs of (a) pion (b) electron samples with the momentum ranging from 0.2GeV/c to 1.6GeV/c

2.5 The performance check

To combine the dE/dx , TOF and EMC information, the likelihood approach [27] is adopted. Firstly, the likelihood value of each subsystem is calculated. Then, the total likelihood value of each hypothesis is calculated by the following formula:

$$L_{tot} = L_{dE/dx} * L_{TOF} * L_{EMC}, \quad (9)$$

where $L_{dE/dx}$ and L_{TOF} represent the likelihood value of dE/dx and TOF subsystems respectively. Finally, the likelihood ratio of electron hypothesis is defined as:

$$lh f_e = \frac{L_e}{L_e + L_\pi}, \quad (10)$$

where L_e and L_π are the total likelihood value of electron and π hypothesis. To check the performance of the e/π separation, both the electron and pion samples are generated with the momentum ranging from 0.2 GeV/c to 1.6 GeV/c, by using single particle generator. Fig. 5(a) shows the electron likelihood ratio distributions of these samples. For a particle to be identified as an electron, we require $lh f_e > 0.5$. Fig. 5(b) shows the combined e/π separation performance using the dE/dx , TOF and EMC systems.

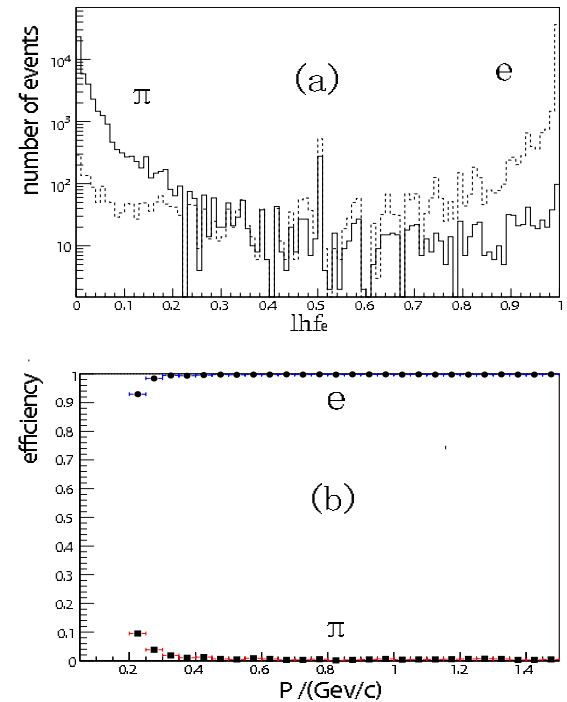


Fig. 5. (a) $lh f_e$ of electron and π samples; (b) performance of e/π separation.

3 Simulation and reconstruction

3.1 The reconstruction of CP tags

For the neutral D meson decays, the main decay modes of $CP+$ eigenstate are K^+K^- , $\pi^+\pi^-$, $K_S\pi^0\pi^0$, $\pi^0\pi^0$, K_SK_S and $\rho^0\pi^0$. The $CP-$ eigenstates decay through the modes $K_S(\pi^0, \rho^0, \eta, \eta', \phi, \omega)$. Considering the branching ratio and the reconstruction efficiency, we only simulated the K^+K^- , $\pi^+\pi^-$ for $CP+$ tagging, and the $K_S(\pi^0, \eta, \eta')$ for $CP-$ tagging.

For selecting the charged tracks, the following selection criteria are adopted:

- 1) All charged tracks must have a good helix fit, and are required to be measured in the fiducial region of MDC;
- 2) Their parameters must be corrected for energy loss and multiple scattering according to the assigned mass hypotheses;
- 3) The tracks not associated with K_S^0 reconstruction are required to be originated from the interaction point(IP).

For reconstructing the $CP+$ eigenstates, two opposite-charged tracks of K or π are selected with the requirements that they are from IP and to pass a common vertex constraint. To identify a track as a π or K , we use the likelihood method to combine the information of dE/dx and TOF with the likelihood fraction of π or K greater than 0.5. Then the beam constrained mass (M_{bc}) of the D meson is used to distinguish the signal and background, and it is defined as:

$$M_{bc} \equiv \sqrt{E_{beam}^2 - (\sum \mathbf{p}_i)^2} = \sqrt{E_{beam}^2 - (\mathbf{p}_D)^2}, \quad (11)$$

where the E_{beam} is the beam energy, the \mathbf{p}_i is the momentum of the i -th track and the $\mathbf{p}_D = \sum \mathbf{p}_i$ is the momentum of the reconstructed D meson.

For tagging the $CP-$ eigenstates, we need to reconstruct the neutral mesons K_S , π^0 , η and η' . The K_S candidates are reconstructed through the decay of $K_S \rightarrow \pi^+\pi^-$. The decay vertex formed by $\pi^+\pi^-$ pair is required to be away from the interaction point, and the momentum vector of $\pi^+\pi^-$ pair must be aligned with the position vector of the decay vertex to the IP. Here we set L_{vtx}/σ_{vtx} to be greater than 2, where L_{vtx} and σ_{vtx} are the measured decay length and the error of the decay length of the K_S . The $\pi^+\pi^-$ invariant mass is required to be consistent with the K_S nominal mass within ± 10 MeV. To identify the neutral tracks, one has to address a number of processes which can produce both real and spurious showers in EMC. The major source of

these “fake photons” arises from hadronic interaction, which can create a “split-off” shower. This shower does not associate with the main shower and may be recognized as a photon. Other sources of fake photons include particle decays, back splash, beam associated background and electronic noise. To reject “fake photons”, the selection criteria for “good photon” include a deposit energy cut, and a spatial cut, which requires that the cluster is isolated from the nearest charged tracks. These “cuts” are set to be $E_\gamma > 40 \text{ MeV}$ and $\Delta_{c\gamma} > 18^\circ$, where E_γ and $\Delta_{c\gamma}$ represent the deposited energy and the crossing angle of the cluster to the nearest charged track, respectively. The neutral pions are reconstructed from $\pi^0 \rightarrow \gamma\gamma$ decays using the photons observed in the barrel and endcap regions of EMC. At the energies of interest, a π^0 decays into two isolated photons. In addition, we also reconstruct η/η' candidates in the modes of $\eta \rightarrow \gamma\gamma$, $\eta \rightarrow \pi^+\pi^-\pi^0$, $\eta' \rightarrow \gamma\rho^0$ and $\eta' \rightarrow \eta\pi^+\pi^-$. For these modes, 3σ consistency with the $\pi^0/\eta/\eta'$ mass is required, followed by a kinematic mass constraint. For $CP-$ eigenstates, the beam constrained mass is also used to select the signal.

Under the environment of BOSS 6.1.0, we simulated $D^0 - \bar{D}^0$ pairs production at the $\psi(3770)$ peak with one D decayed into CP eigenstates and the other D decayed semileptonically. The $CP+$ eigenstates are decayed through $\pi^+\pi^-$ and K^+K^- according to their branching ratios. For $CP-$ eigenstates, the decay modes $K_S\pi^0$, $K_S\eta$ and $K_S\eta'$ are included. In the K_S , π^0 , η and η' decays, the decay modes are listed as follows: $K_S \rightarrow \pi^+\pi^-$, $\pi^0 \rightarrow \gamma\gamma$, $\eta \rightarrow \gamma\gamma$, $\eta \rightarrow \pi^+\pi^-\pi^0$, $\eta' \rightarrow \gamma\rho^0$, and $\eta' \rightarrow \eta\pi^+\pi^-$. For the $CP+$ and $CP-$ eigenstates, we generated 30,000 events for each MC sample. The distributions of the beam constrained mass of D meson are shown in Fig. 6.

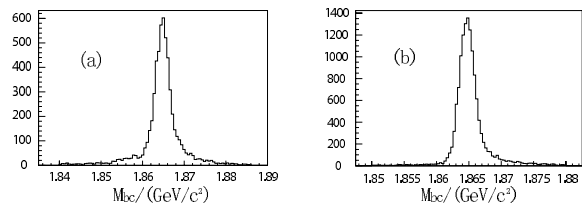


Fig. 6. The M_{bc} of (a) the $CP-$ tags; (b) the $CP+$ tags.

3.2 The reconstruction of semileptonic tags

For tagging the semileptonic decays, we use the decay mode $D^0 \rightarrow K^-e^+\nu_e$. To reconstruct the neutral D meson, good tracks for one electron and one kaon candidate are required. The good track selection criteria are the same as the CP tagging discussed in Section 3.1. The electron and kaon candidates are

also required to be from the IP, and the likelihood ratio of the electron and kaon must both be greater than 0.5. Moreover, the two tracks need to pass a common vertex constraint. After the electron and pion selections, a standard partial reconstruction technique is applied to this semileptonic decay channel with one neutrino associated. Here, we use the “missing mass” (U_{miss}) of neutrino to select the signal candidates. The “missing mass” is defined as follows:

$$U_{miss} \equiv E_{miss} - P_{miss}, \quad (12)$$

where $E_{miss} = E_{D_{tag}} - E_K - E_e$ and $P_{miss} = |\mathbf{p}_{D_{tag}} - \mathbf{p}_K - \mathbf{p}_e|$ are the missing energy and momentum of the neutrino. Here, $E_{K,e}$ and $\mathbf{p}_{K,e}$ are the measured energy and momentum of the selected kaon and electron track. $E_{D_{tag}}$ is the energy of the D meson, which is equal to the beam energy. $\mathbf{p}_{D_{tag}} = -\mathbf{p}_{D_{CP}}$ is the 3-momentum of the D meson, which can be obtained from the reconstructed momentum of the CP tagged D meson. For neutrino, the energy and momentum are equal. Thus, the distribution of U_{miss} must have a mean value at zero. The distribution of U_{miss} is shown in Fig. 7. We apply a 3σ cut on the U_{miss} to select the semileptonic D decays.

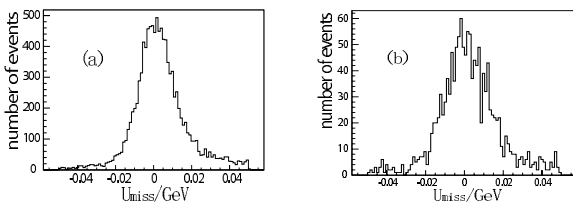


Fig. 7. U_{miss} of ν_e for (a) $CP+$ tags and (b) $CP-$ tags.

4 The sensitivity of y

Table 1 shows the reconstruction efficiency and the number of estimated doubly-tagged events for different simulated decay channels. For $\sim 20\text{fb}^{-1}$ luminosity at $\psi(3770)$ peak, which approximately corresponds to four years data taking at BESIII, about 8.0×10^7 $D^0 - \overline{D}^0$ pairs can be produced. According to the full simulation, about 11000 doubly tagged $CP+$ decays and 9000 doubly tagged $CP-$ decays can be reconstructed.

Table 1. The efficiency and expected events for 8.0×10^7 $D^0 - \overline{D}^0$ decays for different decay channels.

decay mode	efficiency	event estimation
$K^- e^+ \nu_e$		
$K^- K^+, \pi^- \pi^+$	40%	11701
$K^- e^+ \nu_e$		
$K_s \pi^0$	16.8%	7345
$K^- e^+ \nu_e$		
$K_s \eta$	7.7%	715
$K^- e^+ \nu_e$		
$K_s \eta'$	4.7%	953

For a small y , to calculate the σ_y of Equation(6), we ignore the statistical error from single tagged events. Hence, the statistical error of y parameter can be obtained from the following equation:

$$\sigma_y = \frac{1}{2} \times \sqrt{\frac{1}{N_1} + \frac{1}{N_2}}, \quad (13)$$

where N_1 and N_2 represent the reconstructed doubly-tagged $CP+$ and $CP-$ events. As a result, the σ_y is estimated to be 0.007 with $\sim 20\text{fb}^{-1}$ data at $\psi(3770)$ peak in this analysis. Since the double tagging technique is adopted here, the background effect can be ignored comparing to the statistical sensitivity estimated above.

5 Summary

In this paper, we presented a MC study on measuring the $D^0 - \overline{D}^0$ mixing parameter y at the BESIII experiment. Based on a 20fb^{-1} fully simulated MC sample of $\psi(3770)$ resonance decays, we estimated the sensitivity of the y measurement to be 0.007. In this analysis, the double tagging technique was used for reconstructing the D meson pairs. Here, the signal is reconstructed such that one D decays to CP eigenstates and the other D decays semileptonically. The electron identification is essential for this analysis. We improved the e-ID technique for BESIII experiment, which can also be applied to many other important physics topics. Our next step is to include more semileptonic decay modes, such as $D^0 \rightarrow K^* e \nu_e$, into this analysis to improve the sensitivity of y measurement.

References

- 1 Bigi I I, Uraltsev N. Nucl. Phys. B, 2001, **592**: 92
- 2 Burdman G, Shipsey I. Ann. Rev. Nucl. and Part. Sci., 2003, **53**: 431
- 3 Falk A F, Grossman Y, Ligeti Z. Phys. Rev. D, 2002, **65**: 054034
- 4 Falk A F, Grossman Y, Ligeti Z, Petrov A A. Phys. Rev. D, 2004, **69**: 114021
- 5 Staric M et al. (Belle Collaboration). Phys. Rev. Lett., 2007, **98**: 211803
- 6 Aubert B et al. (BABAR Collaboration). Phys. Rev. Lett., 2007, **98**: 211802
- 7 ZHANG L M et al. (Belle Collaboration). Phys. Rev. Lett.,

-
- 2007, **99**: 131803
- 8 Aaltonen T et al. (CDF Collaboration). arXiv:0712.1567
- 9 Aubert B et al. (BABAR Collaboration). arXiv:0712.2249
- 10 Bitenc U et al. (Belle Collaboration). arXiv:0802.2952
- 11 Aubert B et al. (BABAR Collaboration). 2007, **76**: 014018
- 12 SUN Yong-Zhao et al. HEP & NP, 2007, **31**: 423-430 (in Chinese)
- 13 CHENG Xiao-Dong et al. Phys. Rev. D, 2007, **75**: 094019
- 14 Asner D M, Sun W M. Phys. Rev. D, 2006, **73**: 034024
- 15 Asner D M et al. Int. J. Mod. Phys A, 2006, **21**: 5456
- 16 Gronau M, Grossman Y, Rosner J L. Phys. Lett. B, 2001, **508**: 37
- 17 Xing Z Z. Phys. Rev. D, 1997, **55**: 196
- 18 Xing Z Z. Phys. Lett. B, 1996, **372**: 317
- 19 LI Wei-Dong, LIU Huai-Min et al. The Offline Software for the BESIII Experiment, Proceeding of CHEP06, Mumbai, India, 2006
- 20 DENG Zi-Yan et al. HEP & NP, 2006, **30**(5): 371-377 (in Chinese)
- 21 Agostinelli S et al. (Geant4 Collaboration). Nucl. Instrum. Methods, 2003, **506**: 250
- 22 BESIII Design Report, Interior Document in Institute of High Energy Physics, 2004
- 23 QING Gang et al. HEP & NP, 2008, **32**(1): 1-8
- 24 HU Ji-Feng et al. HEP & NP, 2007, **31**(10): 893 (in Chinese)
- 25 Harris F A et al. (BES Collab). arXiv:physics/0606059, 2006
- 26 Bishop C M. Neural Networks for Pattern Recognition. Oxford: Clarendon, 1998; Beale R, Jackson T. Neural Computing: An Introduction. New York: Adam Hilger, 1991
- 27 Carli T, Koblitz B. Nucl. Instrum. Methods A, 2003, **501**: 576-588; Holmström L, Sain R, Miettinen H E. Comput. Phys. Commun., 1995, **88**: 195

A simulation study on the measurement of $D^0 - \bar{D}^0$ mixing parameter y at BESIII *

HUANG Bin^{1,2;1)} ZHENG Yang-Heng^{2;2)} LI Wei-Dong^{1;3)} BIAN Jian-Ming^{1,2}
 CAO Guo-Fu^{1,2} CAO Xue-Xiang^{1,2} CHEN Shen-Jian⁴ DENG Zi-Yan¹ Fu Cheng-Dong^{3,1}
 GAO Yuan-Ning³ HE Kang-Lin¹⁾ HE Miao^{1,2} HUA Chun-Fei⁵ HUANG Xing-Tao¹⁰
 JI Xiao-Bin¹ LI Hai-Bo¹ LIANG Yu-Tie⁶ LIU Chun-Xiu¹ LIU Huai-Min¹
 LIU Qiu-Guang¹ LIU Suo⁷ MA Qiu-Mei¹ MA Xiang^{1,2} MAO Ya-Jun⁶ MAO Ze-Pu¹
 MO Xiao-Hu¹ PAN Ming-Hua⁸ PANG Cai-Ying⁸ PING Rong-Gang¹ QIN Gang^{1,2}
 QIN Ya-Hong⁵ QIU Jin-Fa¹ SUN Sheng-Sen¹ SUN Yong-Zhao^{1,2} WANG Ji-Ke^{1,2}
 WANG Liang-Liang^{1,2} WEN Shuo-Pin¹ WU Ling-Hui¹ XIE Yu-Guang^{1,2} XU Min⁹
 YAN Liang^{1,2} YOU Zheng-Yun⁶ YU Guo-Wei¹ YUAN Chang-Zheng¹ YUAN Ye¹
 ZHANG Chang-Chun¹ ZHANG Jian-Yong¹ ZHANG Xue-Yao¹⁰ ZHANG Yao¹
 ZHU Yong-Sheng¹ ZHU Zhi-Li⁸ ZOU Jia-Heng¹⁰

1 (Institute of High Energy Physics, CAS, Beijing 100049, China)

2 Graduate University of Chinese Academy of Sciences, Beijing 100049, China)

Abstract We established a method on measuring the $D^0 - \bar{D}^0$ mixing parameter y for BESIII experiment at the BEPCII e^+e^- collider. In this method, the doubly tagged $\psi(3770) \rightarrow D^0\bar{D}^0$ events, with one D decays to CP -eigenstates and the other D decays semileptonically, are used to reconstruct the signals. Since this analysis requires good e/π separation, a likelihood approach, which combines the dE/dx , time of flight and the electromagnetic shower detectors information, is used for particle identification. We estimate the sensitivity of the measurement of y to be 0.007 based on a $20fb^{-1}$ fully simulated MC sample.

Key words likelihood, electron identification, $D^0 - \bar{D}^0$ mixing, mixing parameter y

PACS 12.15.Ff, 13.20.Fc, 13.25.Ft, 14.40.Lb, 07.05.Kf

1 Introduction

The mixing between a particle and its antiparticle has been observed experimentally in neutral K , B_d and B_s system. In the Standard Model, however, the mixing rate of the neutral D system is expected in general to be small and long-distance contributions make it difficult to be calculated^[1, 2, 3, 4]. Recently, several measurements^[5, 6, 7, 8, 9] present evidences for $D^0 - \bar{D}^0$ mixing with the significance ranging from 3 to 4 standard deviations. This highlights the need for independent measurements of the mixing parameters. Here, we present a study on measuring the mixing parameter y at BESIII experiment, which takes

advantage of the correlated threshold production of $D^0 - \bar{D}^0$ pairs in e^+e^- collisions.

For the neutral D meson system, two mass eigenstates and flavor eigenstates are not equivalent and can be expressed as the following form of the two quantum states:

$$|D_{A,B}\rangle = p|D^0\rangle \pm q|\bar{D}^0\rangle, \quad (1)$$

with eigenvalues of masses and widths to be $m_{A,B}$ and $\Gamma_{A,B}$. Conventionally, the $D^0 - \bar{D}^0$ mixing is described by two small dimensionless parameters:

$$x \equiv \frac{\Delta m}{\Gamma}, y \equiv \frac{\Delta\Gamma}{2\Gamma}, \quad (2)$$

where $\Delta m \equiv m_A - m_B$, $\Delta\Gamma \equiv \Gamma_A - \Gamma_B$ and $\Gamma \equiv$

Received 29 May 2008, Revised 11 June 2008

* Supported by National Natural Science Foundation of China (10491300,10491303,10735080), Research and Development Project of Important Scientific Equipment of CAS (H7292330S7), 100 Talents Programme of CAS (U-25, U-54,U-612) and Scientific Research Fund of GUCAS(110200M202)

1) E-mail: huangb@ihep.ac.cn

2) E-mail: zhengyh@gucas.ac.cn

3) E-mail: liwd@ihep.ac.cn

$(\Gamma_A + \Gamma_B)/2$. The mixing rate R_M is approximately

$$R_M \approx \frac{x^2 + y^2}{2}. \quad (3)$$

In the limit of CP conservation, the $|D_A\rangle$ and $|D_B\rangle$ denote the CP eigenstates.

The mixing parameters can be measured in several ways. The B -factories measured R_M with semileptonic D^0 decay samples^[10, 11]. Reference^[12, 13] also gave an estimation on the sensitivities of R_M measurement at BESIII. Other attempts^[5, 6, 7, 8, 9] are based on the proper-time measurements of the neutral D meson decays. However, the time-dependent analyse are not possible at symmetric charm factory, which operates at the $\psi(3770)$ resonance. In this analysis, we utilize the quantum-coherent threshold production of $D^0 - \bar{D}^0$ pairs in a state of definite $C = -1$. Applying the kinematics of the process of $e^+e^- \rightarrow \psi(3770) \rightarrow D^0\bar{D}^0$, we can reconstruct both neutral D mesons (double tagging (DT) technique) to obtain clean samples to measure the mixing parameters, the strong phase difference and the CP violation. For the single D^0 meson decays into a CP eigenstate, the time-integrated decay rate can be written as^[14, 15]:

$$\Gamma_{CP\pm} \equiv \Gamma(D^0 \rightarrow f_{CP\pm}) = 2A_{CP\pm}^2 [1 \mp y], \quad (4)$$

where $f_{CP\pm}$ is a CP eigenstate with eigenvalue ± 1 , and $A_{CP\pm} \equiv |\langle f_{CP\pm} | \mathcal{H} | D^0 \rangle|$ is the magnitude of decay amplitude. If we consider the coherent D -pair decays, in which one D decays into CP eigenstates and the other D decays semileptonically, the decay rate of $(D^0\bar{D}^0)^{C=-1} \rightarrow (l^\pm X)(f_{CP\pm})$ is described as^[16, 17, 18]:

$$\Gamma_{l,CP} \equiv \Gamma[(l^\pm X)(f_{CP})] \approx A_{l^\pm X}^2 A_{CP}^2, \quad (5)$$

where $A_{l^\pm X} \equiv |\langle l^\pm X | \mathcal{H} | D^0 \rangle|$. Here, we neglect terms to order y^2 or higher since y is much smaller than unit. We, thus, can derive:

$$y = \frac{1}{4} \left(\frac{\Gamma_{l,CP+}\Gamma_{CP-} - \Gamma_{l,CP-}\Gamma_{CP+}}{\Gamma_{l,CP-}\Gamma_{CP+} - \Gamma_{l,CP+}\Gamma_{CP-}} \right). \quad (6)$$

To measure y at BESIII, only the electron channels are used to reconstruct the semileptonic D^0 decays. In the muon channels, the transverse momentum of muon is too low to be efficiently identified by the BESIII muon detector. Thus, the e/π separation plays an essential role to suppress the backgrounds. Fig. 1 shows the momentum distribution of the electrons from the semileptonic D decays. The momentum distribution of the pions from s quark decays is similar to Fig. 1. As a result, the performance of electron identification (e-ID) will determine the precision of the measurement of y parameter.

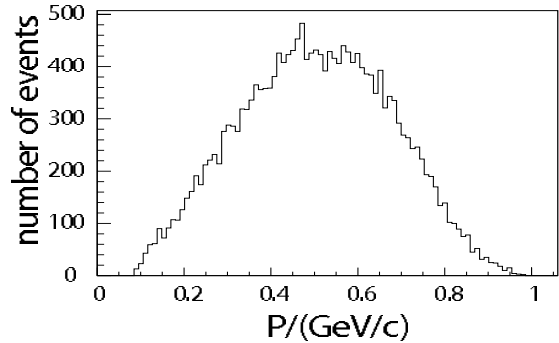


Fig. 1. Momentum of the electron from D^0 semileptonic decays

The designed peak luminosity of BEPCII (Beijing Electron Position Collider) is $10^{33} \text{cm}^{-2} \text{s}^{-1}$ at beam energy $E_{beam} = 1.89 \text{ GeV}$, which is the highest in the tau-charm region ever planned and an unprecedented large number of $\psi(3770)$ events is expected.

This paper is organized as follows: an improved electron identification technique for BESIII is described in Section 2. In Section 3, we describe the method on reconstructing the signals with Monte Carlo (MC) simulation samples. Section 4 presents the estimated sensitivity of y measurement. The summary is presented in Section 5.

2 Electron identification

The BESIII detector operates at BEPCII and consists of a beryllium beam pipe, a helium-based small-celled drift chamber, Time-Of-Flight (TOF) counters for particle identification, a CsI(Tl) crystal electromagnetic calorimeter (EMC), a super-conducting solenoidal magnet with the field of 1 Tesla, and a muon identifier of Resistive Plate Counters (RPC) interleaved with the magnet yoke plates. The BESIII Offline Software System (BOSS)^[19] of version 6.1.0 is used for this analysis. The detector simulation^[20] is based on GEANT4^[21].

The BESIII detector has four subsystems for particle identification: the dE/dx of the main drift chamber (MDC), TOF, EMC and the muon counter. Among them, the dE/dx and the TOF systems are mainly used for hadron separation, the EMC provides information for electron and photon identification, the MDC has good performance on muon identification^[22].

For electron identification, Refs^[23, 24] illustrate the use of dE/dx of MDC and TOF information. Here, an improved e/π separation technique is introduced in the following sections.

2.1 Electromagnetic calorimeter

The BESIII electromagnetic calorimeter^[22, 25] is composed of one barrel and two endcap sections, covering 93% of 4π . There are a total of 44 rings of crystals along the z direction in the barrel, each with 120 crystals. And there are 6 layers in the endcap, with different number of crystals in each layer. The entire calorimeter has 6240 CsI(Tl) crystals with a total weight of about 24 tons. The energy resolution is expected to be 2.5% and the spatial resolution is expected to be 0.6 cm for 1 GeV/c photon.

The primary function of the EMC is to precisely measure the energies and positions of electron and photon. In order to distinguish electron from hadron, we make use of significant differences in energy deposition and the shower shape of different type of the particles.

2.2 Variables used in e-ID

The following variables are used to identify the electron from pion:

- 1) Ratio of the energy measured by the EMC and the momentum of the charged track by the MDC (E/p).

Ratio of the energy measured by the EMC and the momentum of the charged track by the MDC (E/p). When an electron passes through the calorimeter, the electron produces electromagnetic shower and loses its energy by pair-production, Bremsstrahlung and ionizing/exciting atomic electrons. Since the mass of electron is negligible in the energy range of interest, we expect to have the ratio $E/p=1$ within the measurement errors. For hadrons, the E/p is typically smaller than one.

- 2) Lateral shower shape at the EMC.

In order to enhance the separation between the electrons and the interacting hadrons, the lateral shower shape can also be utilized. These variables include: $E_{seed}/E_{3\times 3}$, $E_{3\times 3}/E_{5\times 5}$ and the second-moment. Here the E_{seed} is the energy deposited in the central crystal, the $E_{3\times 3}$ and $E_{5\times 5}$ represent the energy deposit in the 3×3 and 5×5 crystal array, respectively. The second-moment S is defined as

$$S = \frac{\sum_i E_i \cdot d_i^2}{\sum_i E_i}, \quad (7)$$

where E_i is the energy deposit in the i -th crystal, and d_i is the distance between the i -th crystal and the center position of reconstructed shower. Detailed description of E/p and the lateral shower shape can be found in Ref^[23].

- 3) Longitudinal shower shape at the EMC.

The longitudinal shower shape provides additional information for electron identification. The variable $\Delta\phi$, between the polar angles where the track intersects the EMC and the shower center, can be used. The distributions of $\Delta\phi$ for electron and pion are drawn in Fig. 2. The center of electron showers is closer to the impact point of track on EMC since the electron showers reach their maximum earlier than hadrons.

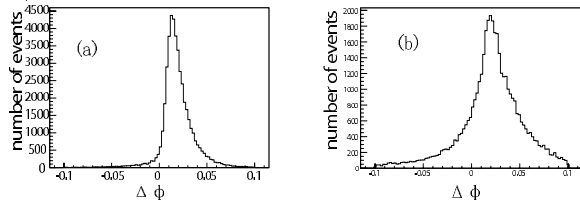


Fig. 2. $\Delta\phi$ of (a) electron (b) pion.

2.3 The correlation between variables

The E/p ratio, lateral shower shape and longitudinal shower shape are all depending on the deposited energy in the crystals. Thus, these variables may be correlated. We calculate the correlation coefficients ρ_{ij} between the E/p , $E_{3\times 3}/E_{5\times 5}$ and $\Delta\phi$ using the function:

$$M_{i,j} = \sum_{i,j} (x_i - \bar{x}_i) \cdot (x_j - \bar{x}_j), \quad \rho_{ij} = \frac{M_{ij}}{\sqrt{M_{ii} \times M_{jj}}}, \quad (8)$$

where i, j are the indices of the variable names. Figure. 3 shows the correlation between any two of the variables of electron and pion, respectively, with the momentum ranging from 0.2 GeV/c to 2.0 GeV/c. Here, the x-axis represents the particle momentum and the y-axis represents the correlation coefficient ρ_{ij} . The distribution indicates strong correlation between the variables.

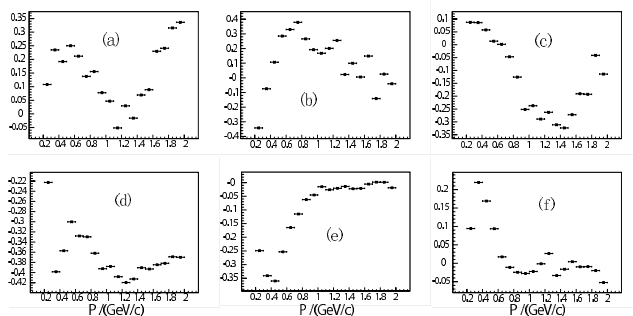


Fig. 3. Correlations between (a) E/p and $E_{seed}/E_{3\times 3}$ of electron; (b) E/p and $E_{3\times 3}/E_{5\times 5}$ of electron; (c) $E_{seed}/E_{3\times 3}$ and $E_{3\times 3}/E_{5\times 5}$ of electron; (d) E/p and $E_{seed}/E_{3\times 3}$ of pion; (e) E/p and $E_{3\times 3}/E_{5\times 5}$ of pion; (f) $E_{seed}/E_{3\times 3}$ and $E_{3\times 3}/E_{5\times 5}$ of pion.

2.4 PID Algorithm

Considering the correlations between the variables, the traditional method for particle identification may be underperforming. In the e-ID, we implement the artificial neural network (ANN) [26] to provide a general framework for estimating non-linear functional mapping between the input variables and the output variable. For the neural network (NN) training, we use the momentum, traverse momentum and other six discriminants (total deposit energy, E_{seed} , $E_{3 \times 3}$, $E_{5 \times 5}$, second moment and $\Delta\phi$) as the input variables. The network we choose has one hidden layer with 16 neurons and one output value. Figure. 4 shows the two-dimension distributions of the output value versus the momentum of the electrons and pions. It is obvious that the distribution of the output value depends on the momentum, especially at low momentum region. Thus, it is unsuitable to apply a single cut on the output value to separate the electrons from the pions. In practice, we construct probability density function (PDF) of the NN output value at every 0.1 GeV/c momentum bin. The PDF is obtained from fitting the nearest 4 bins of the NN output value, with the third-order polynomial function. Then, the PDF value of the NN output can be extracted from the fit. Finally, we make the PID decision by comparing the likelihood values of electron and pion hypothesis.

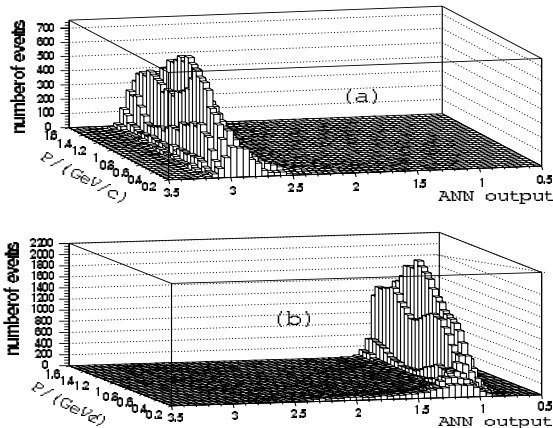


Fig. 4. The NN outputs of (a) pion (b) electron samples with the momentum ranging from 0.2GeV/c to 1.6GeV/c

2.5 The performance check

To combine the dE/dx , TOF and EMC information, the likelihood approach [27] is adopted. Firstly, the likelihood value of each subsystem is calculated. Then, the total likelihood value of each hypothesis is calculated by the following formula:

$$L_{\text{tot}} = L_{dE/dx} * L_{\text{TOF}} * L_{\text{EMC}}, \quad (9)$$

where $L_{dE/dx}$ and L_{TOF} represent the likelihood value of dE/dx and TOF subsystems respectively. Finally, the likelihood ratio of electron hypothesis is defined as:

$$lh f_e = \frac{L_e}{L_e + L_\pi}, \quad (10)$$

where L_e and L_π are the total likelihood value of electron and π hypothesis. To check the performance of the e/π separation, both the electron and pion samples are generated with the momentum ranging from 0.2 GeV/c to 1.6 GeV/c, by using single particle generator. Fig. 5(a) shows the electron likelihood ratio distributions of these samples. For a particle to be identified as an electron, we require $lh f_e > 0.5$. Fig. 5(b) shows the combined e/π separation performance using the dE/dx , TOF and EMC systems.

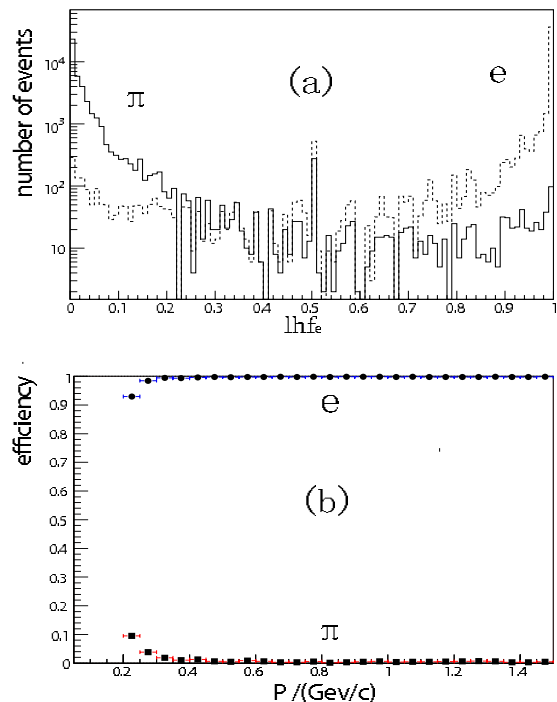


Fig. 5. (a) $lh f_e$ of electron and π samples; (b) performance of e/π separation.

3 Simulation and reconstruction

3.1 The reconstruction of CP tags

For the neutral D meson decays, the main decay modes of $CP+$ eigenstate are K^+K^- , $\pi^+\pi^-$, $K_S\pi^0\pi^0$, $\pi^0\pi^0$, $K_S K_S$ and $\rho^0\pi^0$. The $CP-$ eigenstates decay through the modes $K_S(\pi^0, \rho^0, \eta, \eta', \phi, \omega)$. Considering the branching ratio and the reconstruction efficiency, we only simulated the K^+K^- , $\pi^+\pi^-$ for $CP+$ tagging, and the $K_S(\pi^0, \eta, \eta')$ for $CP-$ tagging.

For selecting the charged tracks, the following selection criteria are adopted:

- 1) All charged tracks must have a good helix fit, and are required to be measured in the fiducial region of MDC;
- 2) Their parameters must be corrected for energy loss and multiple scattering according to the assigned mass hypotheses;
- 3) The tracks not associated with K_S^0 reconstruction are required to be originated from the interaction point(IP).

For reconstructing the $CP+$ eigenstates, two opposite-charged tracks of K or π are selected with the requirements that they are from IP and to pass a common vertex constraint. To identify a track as a π or K , we use the likelihood method to combine the information of dE/dx and TOF with the likelihood fraction of π or K greater than 0.5. Then the beam constrained mass(M_{bc}) of the D meson is used to distinguish the signal and background, and it is defined as:

$$M_{bc} \equiv \sqrt{E_{beam}^2 - (\sum \mathbf{p}_i)^2} = \sqrt{E_{beam}^2 - (\mathbf{p}_D)^2}, \quad (11)$$

where the E_{beam} is the beam energy, the \mathbf{p}_i is the momentum of the i -th track and the $\mathbf{p}_D = \sum \mathbf{p}_i$ is the momentum of the reconstructed D meson.

For tagging the $CP-$ eigenstates, we need to reconstruct the neutral mesons K_S , π^0 , η and η' . The K_S candidates are reconstructed through the decay of $K_S \rightarrow \pi^+\pi^-$. The decay vertex formed by $\pi^+\pi^-$ pair is required to be away from the interaction point, and the momentum vector of $\pi^+\pi^-$ pair must be aligned with the position vector of the decay vertex to the IP. Here we set L_{vtx}/σ_{vtx} to be greater than 2, where L_{vtx} and σ_{vtx} are the measured decay length and the error of the decay length of the K_S . The $\pi^+\pi^-$ invariant mass is required to be consistent with the K_S nominal mass within ± 10 MeV. To identify the neutral tracks, one has to address a number of processes which can produce both real and spurious showers in EMC. The major source of these “fake photons” arises from hadronic interaction, which can create a “split-off” shower. This shower does not associate with the main shower and may be recognized as a photon. Other sources of fake photons include particle decays, back splash, beam associated background and electronic noise. To reject “fake photons”, the selection criteria for “good photon” include a deposit energy cut, and a spatial cut, which requires that the cluster is isolated from the nearest charged tracks. These “cuts” are set to be $E_\gamma > 40$ MeV and $\Delta_{c\gamma} > 18^\circ$, where E_γ and $\Delta_{c\gamma}$ represent the deposited energy and the crossing angle of the cluster to the nearest charged track, respectively.

The neutral pions are reconstructed from $\pi^0 \rightarrow \gamma\gamma$ decays using the photons observed in the barrel and endcap regions of EMC. At the energies of interest, a π^0 decays into two isolated photons. In addition, we also reconstruct η/η' candidates in the modes of $\eta \rightarrow \gamma\gamma$, $\eta \rightarrow \pi^+\pi^-\pi^0$, $\eta' \rightarrow \gamma\rho^0$ and $\eta' \rightarrow \eta\pi^+\pi^-$. For these modes, 3σ consistency with the $\pi^0/\eta/\eta'$ mass is required, followed by a kinematic mass constraint. For $CP-$ eigenstates, the beam constrained mass is also used to select the signal.

Under the environment of BOSS 6.1.0, we simulated $D^0 - \bar{D}^0$ pairs production at the $\psi(3770)$ peak with one D decayed into CP eigenstates and the other D decayed semileptonically. The $CP+$ eigenstates are decayed through $\pi^+\pi^-$ and K^+K^- according to their branching ratios. For $CP-$ eigenstates, the decay modes $K_S\pi^0$, $K_S\eta$ and $K_S\eta'$ are included. In the K_S , π^0 , η and η' decays, the decay modes are listed as follows: $K_S \rightarrow \pi^+\pi^-$, $\pi^0 \rightarrow \gamma\gamma$, $\eta \rightarrow \gamma\gamma$, $\eta \rightarrow \pi^+\pi^-\pi^0$, $\eta' \rightarrow \gamma\rho^0$, and $\eta' \rightarrow \eta\pi^+\pi^-$. For the $CP+$ and $CP-$ eigenstates, we generated 30,000 events for each MC sample. The distributions of the beam constrained mass of D meson are shown in Fig. 6.

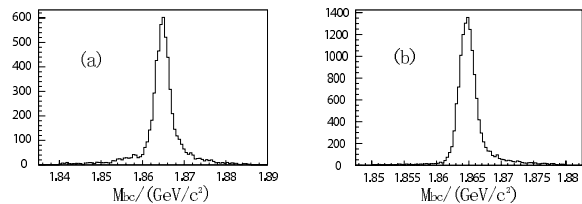


Fig. 6. The M_{bc} of (a)the $CP-$ tags; (b)the $CP+$ tags.

3.2 The reconstruction of semileptonic tags

For tagging the semileptonic decays, we use the decay mode $D^0 \rightarrow K^- e^+ \nu_e$. To reconstruct the neutral D meson, good tracks for one electron and one kaon candidate are required. The good track selection criteria are the same as the CP tagging discussed in Section 3.1. The electron and kaon candidates are also required to be from the IP, and the likelihood ratio of the electron and kaon must both be greater than 0.5. Moreover, the two tracks need to pass a common vertex constraint. After the electron and pion selections, a standard partial reconstruction technique is applied to this semileptonic decay channel with one neutrino associated. Here, we use the “missing mass” (U_{miss}) of neutrino to select the signal candidates. The “missing mass” is defined as follows:

$$U_{miss} \equiv E_{miss} - P_{miss}, \quad (12)$$

where $E_{miss} = E_{D_{tag}} - E_K - E_e$ and $P_{miss} = |\mathbf{p}_{D_{tag}} - \mathbf{p}_K - \mathbf{p}_e|$ are the missing energy and momentum of

the neutrino. Here, $E_{K,e}$ and $\mathbf{p}_{K,e}$ are the measured energy and momentum of the selected kaon and electron track. $E_{D_{tag}}$ is the energy of the D meson, which is equal to the beam energy. $\mathbf{p}_{D_{tag}} = -\mathbf{p}_{D_{CP}}$ is the 3-momentum of the D meson, which can be obtained from the reconstructed momentum of the CP tagged D meson. For neutrino, the energy and momentum are equal. Thus, the distribution of U_{miss} must have a mean value at zero. The distribution of U_{miss} is shown in Fig. 7. We apply a 3σ cut on the U_{miss} to select the semileptonic D decays.

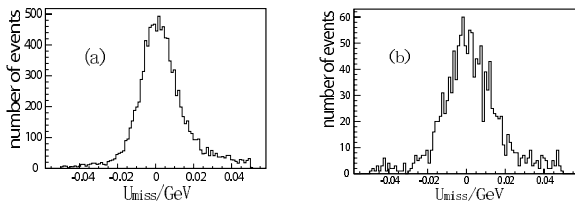


Fig. 7. U_{miss} of ν_e for (a) $CP+$ tags and (b) $CP-$ tags.

4 The sensitivity of y

Table 1 shows the reconstruction efficiency and the number of estimated doubly-tagged events for different simulated decay channels. For $\sim 20\text{fb}^{-1}$ luminosity at $\psi(3770)$ peak, which approximately corresponds to four years data taking at BESIII, about 8.0×10^7 $D^0 - \bar{D}^0$ pairs can be produced. According to the full simulation, about 11000 doubly tagged $CP+$ decays and 9000 doubly tagged $CP-$ decays can be reconstructed.

Table 1. The efficiency and expected events for 8.0×10^7 $D^0 - \bar{D}^0$ decays for different decay channels.

decay mode	efficiency	event estimation
$K^-e^+\nu_e$		
$K^-K^+, \pi^-\pi^+$	40%	11701
$K^-e^+\nu_e$		
$K_s\pi^0$	16.8%	7345
$K^-e^+\nu_e$		
$K_s\eta$	7.7%	715
$K^-e^+\nu_e$		
$K_s\eta'$	4.7%	953

For a small y , to calculate the σ_y of Equation(6), we ignore the statistical error from single tagged events. Hence, the statistical error of y parameter can be obtained from the following equation:

$$\sigma_y = \frac{1}{2} \times \sqrt{\frac{1}{N_1} + \frac{1}{N_2}}, \quad (13)$$

where N_1 and N_2 represent the reconstructed doubly-tagged $CP+$ and $CP-$ events. As a result, the σ_y is estimated to be 0.007 with $\sim 20\text{fb}^{-1}$ data at $\psi(3770)$ peak in this analysis. Since the double tagging technique is adopted here, the background effect can be ignored comparing to the statistical sensitivity estimated above.

5 Summary

In this paper, we presented a MC study on measuring the $D^0 - \bar{D}^0$ mixing parameter y at the BESIII experiment. Based on a 20fb^{-1} fully simulated MC sample of $\psi(3770)$ resonance decays, we estimated the sensitivity of the y measurement to be 0.007. In this analysis, the double tagging technique was used for reconstructing the D meson pairs. Here, the signal is reconstructed such that one D decays to CP eigenstates and the other D decays semileptonically. The electron identification is essential for this analysis. We improved the e-ID technique for BESIII experiment, which can also be applied to many other important physics topics. Our next step is to include more semileptonic decay modes, such as $D^0 \rightarrow K^*e\nu_e$, into this analysis to improve the sensitivity of y measurement.

References

- 1 Bigi I I, Uraltsev N. Nucl. Phys. B, 2001, **592**: 92
- 2 Burdman G, Shipsey I. Ann. Rev. Nucl. and Part. Sci., 2003, **53**: 431
- 3 Falk A F, Grossman Y, Ligeti Z. Phys. Rev. D, 2002, **65**: 054034
- 4 Falk A F, Grossman Y, Ligeti Z, Petrov A A. Phys. Rev. D, 2004, **69**: 114021
- 5 Staric M et al. (Belle Collaboration). Phys. Rev. Lett., 2007, **98**: 211803
- 6 Aubert B et al. (BABAR Collaboration). Phys. Rev. Lett., 2007, **98**: 211802
- 7 ZHANG L M et al. (Belle Collaboration). Phys. Rev. Lett., 2007, **99**: 131803
- 8 Aaltonen T et al. (CDF Collaboration). arXiv:0712.1567
- 9 Aubert B et al. (BABAR Collaboration). arXiv:0712.2249
- 10 Bitenc U et al. (Belle Collaboration). arXiv:0802.2952
- 11 Aubert B et al. (BABAR Collaboration). 2007, **76**: 014018
- 12 SUN Yong-Zhao et al. HEP & NP, 2007, **31**: 423-430 (in Chinese)
- 13 CHENG Xiao-Dong et al. Phys. Rev. D, 2007, **75**: 094019
- 14 Asner D M, Sun W M. Phys. Rev. D, 2006, **73**: 034024
- 15 Asner D M et al. Int. J. Mod. Phys A, 2006, **21**: 5456

-
- 16 Gronau M, Grossman Y, Rosner J L. Phys. Lett. B, 2001, **508**: 37
 - 17 Xing Z Z. Phys. Rev. D, 1997, **55**: 196
 - 18 Xing Z Z. Phys. Lett. B, 1996, **372**: 317
 - 19 LI Wei-Dong, LIU Huai-Min et al. The Offline Software for the BESIII Experiment, Proceeding of CHEP06, Mumbai, India, 2006
 - 20 DENG Zi-Yan et al. HEP & NP, 2006, **30**(5): 371-377 (in Chinese)
 - 21 Agostinelli S et al. (Geant4 Collaboration). Nucl. Instrum. Methods, 2003, **506**: 250
 - 22 BESIII Design Report, Interior Document in Institute of High Energy Physics, 2004
 - 23 QING Gang et al. HEP & NP, 2008, **32**(1): 1-8
 - 24 HU Ji-Feng et al. HEP & NP, 2007, **31**(10): 893 (in Chinese)
 - 25 Harris F A et al. (BES Collab). arXiv:physics/0606059, 2006
 - 26 Bishop C M. Neural Networks for Pattern Recognition. Oxford: Clarendon, 1998; Beale R, Jackson T. Neural Computing: An Introduction. New York: Adam Hilger, 1991
 - 27 Carli T, Koblitz B. Nucl. Instrum. Methods A, 2003, **501**: 576-588; Holmström L, Sain R, Miettinen H E. Comput. Phys. Commun., 1995, **88**: 195